JOURNAL OF MATERIALS SCIENCE 10 (1975) 481–492

Storage and loss moduli in discontinuous composites

D. McLEAN, B. E. READ
National Physical Laboratory, Teddington, Middlesex, UK

The paper deals with viscoelastic, rubber-like material unidirectionally reinforced with discontinuous fibres. The longitudinal storage modulus is calculated not only from an equation based on an existing force balance treatment but also from the elastic strain energy stored in matrix and fibres, using two different models to derive the stress and strain distributions from which the stored energy is calculated. There is very good agreement between all the calculations. The energy calculations reveal that loss modulus is also greatly increased by discontinuous reinforcement and enable its value to be estimated. Experiments on storage and loss modulus are reported and show that the calculations underestimate storage modulus and overestimate loss modulus. In both cases the factor of error ~ 2, and arises because the amplified matrix strain is underestimated and is partly hydrostatic; the hydrostatic strain is non-dissipative and therefore does not contribute to the loss modulus. Discontinuous reinforcement can increase loss modulus as well as storage modulus by more than 100 times, and this should help sound and vibration deadening. An estimate is made of the wide ratio of compliance ÷ breaking strength available with discontinuous but not with continuous reinforcement, which opens up new design latitude for components hitherto reinforced with continuous fibres.

1. Introduction

In this environmentally conscious age, loss modulus is as important as storage modulus because it measures sound and vibration deadening capacity. This paper shows experimentally and theoretically that discontinuous reinforcement of a rubber-like viscoelastic matrix can produce a large increase in loss modulus as well as in storage modulus in the axial direction. The calculations relate also to another problem. Tyres, belts, and hosepipes are currently reinforced with continuous fibres, which makes the ratio of compliance to breaking strength invariant for a given fibre material. With discontinuous fibres the ratio can be varied and the range available is calculated. A variable ratio would give more latitude in the design of these pieces of equipment.

Existing calculations of the storage modulus of discontinuous composites [1, 2] have been based on the method introduced by Cox [3]. In this method the stress or strain distribution in a given fibre and surrounding matrix are first calculated from the equations of elastic force equilibrium. The modulus is then estimated from the average fibre stress resulting from an applied matrix strain or from some average strain in the matrix produced by an applied load. Owing to the complexity of such calculations, certain stress components are often neglected in the basic model, leading to approximations in the derived stress fields, and further approximations are introduced in the definition of average stress or strain. There is a further approximation of unknown magnitude because the idealized fibre distributions for which the calculations are made differ from the irregular distribution in practical discontinuous composites. In general it is difficult to assess not only the magnitude of these approximations but also their sense. Alternative procedures are presented here which rely on strain energy calculations. A geometrical argument [4] shows that shear strain is greatly amplified in reinforced matrix as compared with unreinforced and on this basis approximate calculations are made of the strain energy in matrix and fibres when a sample is stretched. These strain energies are also calculated using the strain distribution deduced here from Cox's force-balance treatment. Because energies are

additive, the sense of the approximational error is clear; moreover, the shear strain amplification makes it immediately obvious that loss modulus as well as storage modulus is greatly increased by discontinuous reinforcement.

The paper, therefore, gives calculations and measurements of loss and storage modulus in the longitudinal direction and indicates the range of breaking strength ÷ compliance offered by discontinuous reinforcement.

2. Calculation of storage modulus

2.1. Geometrical model

When a discontinuous reinforced sample is stretched, there are two distinguishable contributions to the sample extension ϵ: (1) the fibres become extended and contribute amount ϵ_f'; (2) in addition, the fibres move relatively to each other in a longitudinal direction; the resulting shear in the matrix contributes ϵ_m' to the sample strain. Then

$$\epsilon = \epsilon_m' + \epsilon_f' . \qquad (1)$$

In order to find ϵ for a given stress σ, and thus the composite moduli, ϵ_m' and ϵ_f' need to be determined.

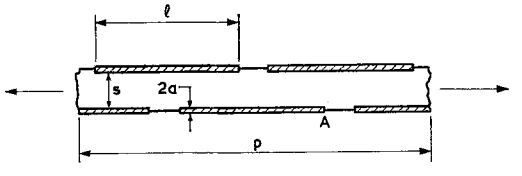

Figure 1

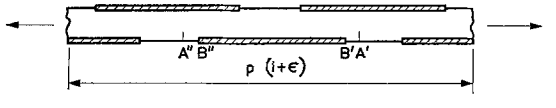

Figure 2

Figures 1 and 2 Schematic diagram of piece of composite before and after an extension ϵ.

One calculation of ϵ_m' depends on geometrical arguments [4], the relevant part of which is briefly repeated. Consider the piece of aligned fibre reinforced material shown in Figs. 1 and 2. Under tensile loading parallel to the fibres this piece of material increases in length from p in Fig. 1 to $p(1 + \epsilon)$ in Fig. 2, the stress/strain curve rising along OC in Fig. 3. A part ϵ_m' of this extension is caused by relative displacement between matrix and fibres and makes the contribution in Fig. 3 indicated by OM. By symmetry, the relative displacement is zero at the centre of the fibre but at the fibre end a point in the matrix such as A (Fig. 1) moves away from the end to A′ (Fig. 2) and between matrix and fibre there is relative displacement A′B′ = $\epsilon_m' l/2$, where l is the fibre length. At the opposite end there is an equal amount A″B″ of relative displacement but in the opposite sense. Assuming that the relative displacement increases linearly from fibre centre to fibre end the average relative displacement is $\epsilon_m' l/4$.

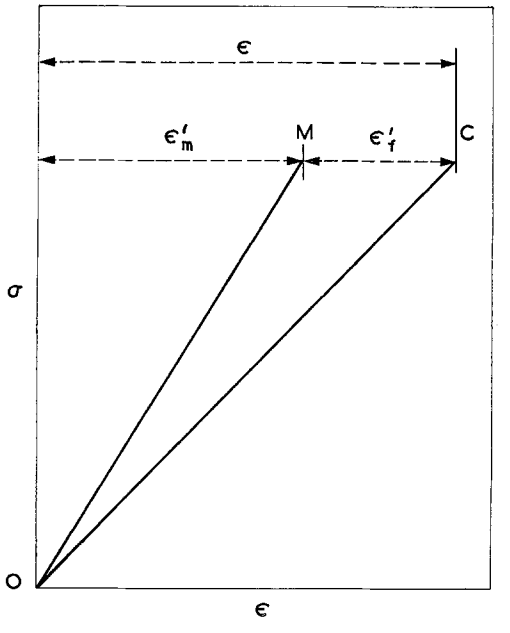

Figure 3 Stress-strain diagram. ϵ_m' is the sample extension associated with shear strain amplification in the matrix. ϵ_f' is the (additional) sample extension associated with extension of the fibres.

This last assumption requires the fibre strain ϵ_f to be substantially less than the applied strain ϵ even at the fibre centre; otherwise ϵ_m' would be zero opposite a central stretch of each fibre. In the material to which the calculations are applied it will be seen in the discussion that this condition is satisfied.

The fibre/matrix bond is significant for the magnitude of ϵ_m'. At one extreme, which is more likely in practice, suppose there is such strong adhesion of matrix to fibre that no sliding can take place at the interface between them. To accommodate the relative displacement a shear strain must then occur in the matrix. By

symmetry, along a centre line in the matrix, i.e. along a line joining the arrows in Figs. 1 and 2, there is the relative displacement parallel to the fibres just indicated. If s is the transverse spacing between fibres (Fig. 1), the consequential average shear strain γ parallel to the fibres is $\gamma = \epsilon_m' l/2s$. In unreinforced matrix the shear strain would be $\gamma_u = 2\epsilon_m'$ (the Tresca value). The shear strain amplification γ/γ_u is, therefore, $l/4s$. If the matrix is Hookean the elastic strain energy stored in the volume V_m of matrix contained in unit volume of composite is consequently, $V_m(l/4s)^2 \times$ that stored in unit volume of unreinforced matrix extended by the same amount. Hence, if the same *stress* σ is applied to reinforced and unreinforced, the work stored is $V_m(l/4s)^2 \times$ less in the former than in the latter, and in unit volume of composite is thus

$$W_m = \frac{8\sigma^2}{E_m V_m (l/s)^2} \cdot \qquad (2)$$

The relative displacement between matrix and fibre may alternatively be accommodated entirely or partly by sliding at matrix/fibre interfaces if adhesion there is weak. Then ϵ_m' and W_m are both increased for given σ. Further, stress transfer to the fibres is weakened and the latter's contribution to the breaking strength is diminished. Sliding thus diminishes tensile modulus and strength and it will be assumed to be avoided by adequate adhesion. Sliding can, however, help damping as indicated later.

The other contribution to the strain, ϵ_f', arises because a tensile stress σ_f is induced in the fibres when the sample is extended. The contribution ϵ_f' produces in Fig. 3 the difference between OC and OM. σ_f varies along a fibre length, and if the matrix is Hookean is given by Equation 11 of [4] as

$$\sigma_f = \frac{\sigma}{V_f}\left(1 - \frac{4x^2}{l^2}\right) \qquad (3)$$

where V_f is the volume fraction of fibres, x is the distance from the mid-point, and it has been assumed that at its mid-point a fibre carries the full applied load, i.e. the stress there is σ/V_f, and the adjoining matrix carries zero longitudinal stress. By averaging $\sigma_f^2/2E_f$ (E_f being the fibre modulus) along the fibre length the strain energy stored in the fibres is found to be

$$W_f = \frac{4\sigma^2}{15E_f V_f} \cdot \qquad (4)$$

*In [4] the factor 2 was omitted from the numerator.

The matrix is, of course, also extended by the amount ϵ_f' in addition to ϵ_m' but no strain amplification is now involved, so that for the compliant rubbery matrices in question the corresponding energy and stress terms are negligible. This is why the stress at the mid-point of a fibre can be taken as σ/V_f.

The total strain energy $W_c = W_m + W_f$. Further, $W_c\ [= \frac{1}{2}\sigma(\epsilon_m' + \epsilon_f')] = \sigma^2/2E_c$ whence

$$\frac{1}{E_c} = \frac{16}{E_m V_m (l/s)^2} + \frac{8}{15E_f V_f} \cdot \qquad (5)$$

Using Equation 5 E_c is plotted versus V_f in Fig. 4 as the solid line for the polymer-carbon fibre composite on which the experiments described below were performed: $E_m = 0.03$ GN m^{-2}, $E_f = 400$ GN m^{-2}, and the value of l/s assuming a square array of fibres on a transverse section is

$$\frac{l}{s} = \frac{2rV_f}{\sqrt{(\pi V_f)} - 2V_f} \cdot \qquad (6)^*$$

where the fibre-aspect ratio $r = 112$. Since Equation 5 does not apply when $V_f \to 0$ because a term for unreinforced matrix has not been included, in Fig. 4 E_c was calculated only between $V_f = 0.2$ and $V_f = 0.01$ and was continued by eye from the latter point to the experimental value of E_m at $V_f = 0$.

2.2. Force-balance model

For comparison, a calculation from an existing force-balance model was also made. Cox's model [3] was chosen since discussion subsequent to his paper has not obviously produced any improvement as far as calculation of the longitudinal modulus of a discontinuously reinforced composite is concerned. The model is depicted in Fig. 5. Each fibre is assumed to be surrounded by a cylinder of matrix, radius y_1, the external surface of which is extended by the composite strain ϵ, and a force balance method is then used to calculate the stress in the fibre, giving longitudinal modulus as (Equation 32 of [3]).

$$E_c = E_f V_f \left[1 - \frac{\tanh \beta l/2}{\beta l/2}\right] \qquad (7)$$

where $\beta = \sqrt{[2G_m/E_f a^2 \ln(y_1/a)]}$ (see Appendix), G_m being the shear modulus of the matrix. E_c calculated from Equation 7 assuming $G_m = E_m/3 = 0.01$ GN m^{-2} is indistinguishable in Fig. 4 from the previous energy calculation (Equation 5). In the calculation from Equation 7, y_1 was

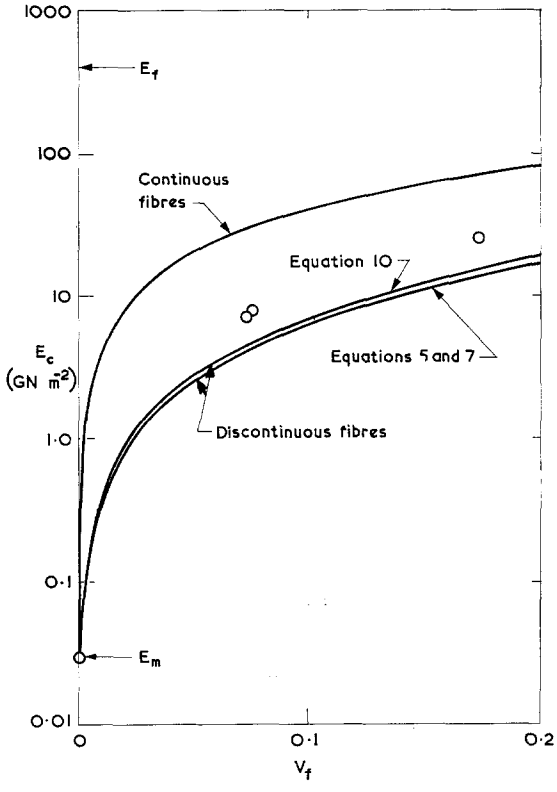

Figure 4 The lower curves show the calculated influence of V_f on longitudinal composite modulus E_c in the case of discontinuous reinforcement. The upper curve relates to continuous reinforcement when $E_f \gg E_m$. The circles are experimental measurements. Carbon fibres in soft polymer.

taken as half the centre-to-centre spacing. However, following Cox, a regular hexagonal array of fibres on a transverse section was assumed; this yields $y_1/a = 0.952/V_f^{\frac{1}{2}}$ and $l/s = 2rV_f/(1.905V_f^{\frac{1}{2}} - 2V_f)$, which is little different from Equation 6. Since Equation 7 gives $E_c = 0$ at $V_f = 0$, the calculation was again made only down to $V_f = 0.01$ and continued by eye to the value of E_m at $V_f = 0$.

From the model we may calculate the shear strain in the matrix and the tensile strain in the fibres which arise when the sample is extended, so that the strain energies W_m and W_f can be deduced and E_c hence calculated from the strain energy. It seemed worth doing this, especially as a calculation of loss modulus would also then become possible.

In Fig. 5 a cross-section such as XYZ which is plane in the unstressed condition becomes

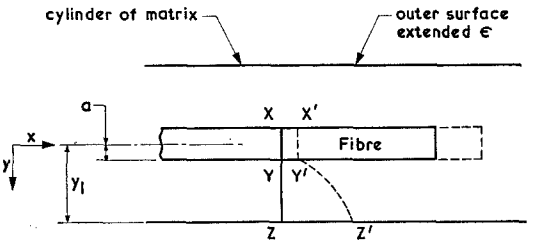

Figure 5 Unit cell of Cox's model. The plane XYZ becomes X'Y'Z' when a stress is applied.

X'Y'Z' when an external longitudinal tensile stress is applied. In the Appendix it is shown that the resultant matrix shear stress τ and shear strain γ at a radial distance y from the fibre centre line are $\tau = \tau_0 a/y$ with of course $\gamma = \tau/G_m$; τ_0 is the shear stress at the fibre-matrix interface and varies with x. It might be noted that τ and γ do not vanish at any point between adjacent fibres (unless $\tau_0 = 0$) as in reality they sometimes must; the reason is the model's neglect of tensile stresses in the matrix. In the Appendix it is further shown that

$$\tau = \frac{a^2 E_f \epsilon \beta \sinh\beta\left(\frac{l}{2} - x\right)}{2y \cosh\frac{\beta l}{2}}$$

where ϵ is the longitudinal composite strain as before. The shear strain energy stored in the cylinder of matrix of radius y_1 surrounding each fibre is

$$w_m = \int_{y=a}^{y_1} \int_{x=0}^{l/2} \int_{\theta=0}^{2\pi} \tau\gamma\, y\, dy\, dx\, d\theta,$$

where θ is the azimuthal angle in the plane perpendicular to the plane of the paper in Fig. 5. The strain energy W_m in the volume V_m of matrix contained in unit volume of composite is $V_m w_m/\pi\, l(y_1^2 - a^2)$ and works out to

$$W_m = \frac{\epsilon^2 V_m E_f(\sinh\beta l - \beta l)}{2\beta l(y_1^2/a^2 - 1)(1 + \cosh\beta l)}. \quad (8)$$

The strain energy in the fibres can also be calculated. Cox finds the longitudinal fibre stress to be

$$\sigma_f = \epsilon E_f\left[1 - \frac{\cosh\beta(l/2 - x)}{\cosh\beta l/2}\right]$$

and the fibre strain is of course $\epsilon_f = \sigma_f/E_f$. Hence the strain energy stored in one fibre is

$$w_f = \int_0^{l/2} \pi a^2 \sigma_f \epsilon_f dx .$$

The strain energy W_f in the volume V_f of fibres contained in unit volume of composite is, therefore,

$$W_f = \frac{\epsilon^2 E_f V_f}{\beta l} \left[\frac{\beta l(\cosh \beta l + 2) + \sinh \beta l}{2(\cosh \beta l + 1)} - 2 \tanh \beta l/2 \right] \cdot \quad (9)$$

E_c can be found from

$$E_c = 2W_c/\epsilon^2 = 2(W_m + W_f)/\epsilon^2 . \quad (10)$$

E_c has been calculated from Equation 10 using $G_m = 0.01$ GN m^{-2} and the same composite parameters as before and the result is plotted in Fig. 4. The new values are about 1.1 times larger than those given by Equation 7 (e.g. 1.09 at $V_f = 0.1$) and thus slightly closer to the experimental values.

3. Measurement of storage modulus

The experimental composite samples consisted of unidirectionally aligned chopped carbon fibres (type I, high modulus) in a high damping matrix of uncross-linked polymer. The matrix polymer was obtained from Hoechst Chemicals and was designated VP71. It had a soft rubber-like consistency at room temperature and flowed readily under load so that specimens in strip form were unable to support their own weight. They were therefore studied in the form of layers on the surface of steel strips. Two-layered polymer-steel specimens were prepared by placing polymer on the surface of steel strips edged with aluminium foil and heating to 120°C. As the polymer was liquid-like at this temperature, it readily flowed into a layer of uniform thickness and air bubbles were slowly expelled. The aluminium foil edging was subsequently removed.

To make the composite samples, oriented chopped carbon fibre mats of thickness 1.8 mm were used containing 11.8 wt%VP71 as a binder. These mats were kindly prepared by Fothergill and Harvey Ltd using a published process [5]. Since specimens of the desired V_f (i.e. < 0.2) were unable to support their own weight, they were also prepared as layers on the surface of steel strips. A suitable piece of mat was placed on a steel strip edged with aluminium foil so that its fibres were oriented in the longitudinal direction of the strip. A calculated quantity of VP71 was roughly pressed into strip form and placed on top of the mat. After heating to 120°C the polymer penetrated the mat to form a composite specimen which adhered to the steel surface. As an alternative to heating, it was also found that the polymer penetrated the mat if exposed to acetone vapour in a desiccator, as the acetone vapour had the effect of producing a fairly thick polymer solution; the acetone solvent could subsequently be removed by slow evaporation. No difference has so far been found between the properties of composites prepared by the two methods. Composite samples with V_f approximately equal to 0.07 and 0.17 respectively have been made.

Some examination was made to characterize the samples. In the case of those with $V_f = 0.07$, the values of V_f calculated from the density of the final samples agreed with the values calculated from the initial weights of VP71 and carbon fibres, indicating that no voids were present. The samples with $V_f = 0.17$, however, were found from a comparison of measured and estimated densities to contain between 17% and 38% voids which were not entirely removed by pressing the specimens. The results quoted later relate to zero void content as determined by extrapolating from measurements at several void contents. In order to measure fibre lengths, small pieces of mat were stirred in acetone to dissolve the VP71 and disperse the fibres, which were collected on filter paper and photographed at × 10. In all 314 fibres were measured, their lengths ranged from 0.05 to 2.8 mm, with an arithmetic mean of 0.81 mm. Some breakage must have occurred during preparation of the mats since the original fibres were uniformly 3 mm long. To measure fibre diameters, some oriented fibre specimens were prepared by incorporating into strips of the mat an epoxy resin which cured to a rigid matrix. Cross-sections of these specimens were photographed in an optical microscope after polishing. Among the 200 fibres measured in this way, the diameters ranged from 4.30 to 9.1 μm with an arithmetic mean of 7.2 μm. The ratio r of average fibre length to average fibre diameter in the composite samples was therefore equal to 112.

The moduli of the polymer and composite samples were determined from the difference in resonance frequency of a steel strip with and without a layer of sample attached. Since VP71 adheres well to steel, the method described was well suited to making the necessary test pieces

and was partly chosen for this reason. The test pieces, which were 180 mm long and 12.7 mm wide, were suspended by fine nylon filaments at their nodal points and forced at one end into flexural vibrations by a magnetic transducer fed by a variable frequency oscillator. The amplitude of vibration was determined at the other end by a proximitor, the output of which was fed through an amplifier to a recorder. Measurements were made of the various resonant frequencies $f_n (n = 1, 2, 3 \ldots)$ at which the vibration amplitude was a maximum. Two steel samples were employed, having respectively thicknesses of about 1 mm and 2.5 mm, and these exhibited fundamental resonant frequencies f_1 of about 169 and 424 Hz respectively.

Assuming that the flexural vibration induces only longitudinal tension and compression and no longitudinal shear, simple beam theory gives the bending stiffness B (defined as bending moment ÷ curvature) $= 4\pi^2 M X^3 f_n^2 / K_n^4$, where M is the mass and X the length of the two-layered strip and $K_n = 4.730$ for the fundamental resonance ($n = 1$). Schwarzl's [6] analysis of two-layered beams was used for determining the modulus E_C of the sample layer from the measured values of bending stiffness, thickness ratio of the two layers and modulus E_S of steel alone. The analysis was modified because the widths I_S and I_C of the steel and the adherent composite differed by a few per cent owing to the lateral contraction of the surface layers on cooling. For Schwarzl's ratio E_C/E_S, the ratio $E_C I_C / E_S I_S$ was substituted throughout and I_S was included as a factor in the expression for the bending stiffness of the two-layered strip. Young's modulus for the unreinforced polymer was determined over a frequency range by measuring the lowest four resonant frequencies (f_1 to f_4) with polymer layers on each of the two steel strips. The value of E_m calculated as described increased from 0.021 GN m^{-2} at 143 Hz to 0.075 GN m^{-2} at 2181 Hz. For the composite specimens, the corresponding value E_C decreased somewhat with increasing resonant frequency, probably because some longitudinal shear deformation occurred at the higher modes owing to the large ratio of tensile to shear moduli in the composite samples. As the errors associated with any shear effects are a minimum at the fundamental mode the moduli obtained at the lowest resonant frequency f_1 are presented here for the composite specimens. Taking into account the large length/thickness ratios (> 100) of the composite layers, errors of less than 7% are estimated for the E_C values on the basis of the theory of Goens [7]. The moduli obtained from the fundamental frequencies around 250 Hz are shown in Fig. 4. Also shown at $V_f = 0$ is the polymer modulus of 0.03 GN m^{-2} which was obtained at 250 Hz from the modulus-frequency plot. The theoretical curves in Fig. 4 run fairly close to the experimental composite values, indicating moduli about two times smaller than the latter.

4. Special case

A rigorous calculation has been made by Ferriss [8] for certain cases and is equivalent to an exact experiment in these cases. A comparison between Ferriss and the previous calculations is therefore another test of the accuracy of the latter.

Ferriss' solution describes flow rate when the matrix material has linear viscosity, is reinforced with infinitely thin and inextensible lamellae, and plane strain under longitudinal tensile stress is in question. Since the basic equations for this situation have the same form as those of linear elasticity the solution also describes strain as a function of tensile stress when the matrix material obeys the laws of linear elasticity and plane strain is also in question; this is the analogy pointed out by Rayleigh [9]. Ferriss' Equation 35, therefore, gives the tensile stress required to produce unit strain in material reinforced with parallel lamellae, the comparable stress in reinforced material being $\bar{\sigma}_x / 4\eta$, in the terminology of Equation 35. These stresses are equal to the moduli and their reciprocals to the compliances.

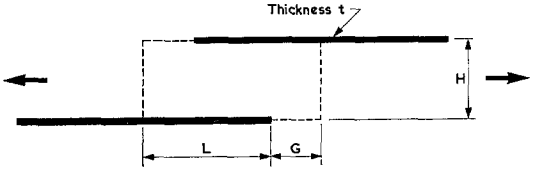

Figure 6 Indicating nomenclature used in the rigorous calculation concerning hard, infinitely thin lamellae in a soft matrix. The dashed lines indicate Ferriss' unit cell. L is half the length of a lamella.

Since reinforcement with lamellae is in question the simplest comparison is with Equation 5, which is expected to apply with about equal accuracy to lamellar and cylindrical

fibres, using for l/s the appropriate ratio indicated below. It is desirable to make the comparison for practically interesting situations so far as this is possible with infinitely thin lamellae, which requires that these situations be expressed in terms of the parameters used in the exact calculation. These are indicated in Ferriss' "unit cell" illustrated in Fig. 6, where L is half a length of a lamella, i.e. $l/2$ in the notation of Fig. 1. The calculations give E_c/E_m as a function of $R = L/(L + G)$ for various values of $K = (L + G)/H$; G is indicated in Fig. 6. For reasonable overlap of adjacent lamellae, R should lie between, say, 0.7 and 1.0. Further,

$$V_f = \frac{Lt}{(L + G)H} = \frac{L^2t(L + G)}{(L + G)^2LH} = \frac{2R^2K}{r},$$

where r is the lamellae aspect ratio, $2L/t$, whence $K = rV_f/2R^2$. Given that the useful upper and lower limits of R^2 are 1.0 and 0.49, the interesting range of K then lies between $rV_f/2$ and rV_f. The interesting range of V_f is mainly between 0.01 and 0.2, while $r > 100$ in order that the lamellae contribute efficiently to the breaking strength (see below). Now l/s, to use the nomenclature of this paper, $= 2L/(H - t)$ in the nomenclature of [8] and $V_f = Lt/[H(L + G)]$ so that $t/H = V_f/R$. Hence

$$l/s = \frac{2L/H}{(1 - t/H)} = \frac{2RK}{1 - V_f/R},$$

which enables Equation 5 to be expressed in terms of Ferriss' parameters.

The ratios E_c/E_m calculated according to Equation 5 and [8] are given in Table I for several conditions. To remind the reader again, the reinforcing lamellae are assumed to be inextensible so that in Equation 5 the second term is zero.

The calculation according to [8] is exact when $t = 0$. It is therefore most accurate for small V_f and large r, for which condition Equation 5 tends almost exactly to half the correct value, as it does in Fig. 4.

It might be remarked that, for given r and V_f, the results in Table I, which relate to lamellar reinforcement, differ markedly from those which would be calculated for rod reinforcement, as can be seen by making comparisons between Table I and Fig. 4. The reason is that l/s is considerably smaller for lamellar than for cylindrical reinforcement at equal r and V_f. The geometrical model thus copes quite well with the substantial difference between lamellar and rod reinforcement.

TABLE I Comparison of $E_c/E_m = C_m/C_c$ calculated in different ways

r	R	K	[8]	Equation 5
V_f0.01				
162	0.9	1.0	2.3	0.2
256	0.8	2.0	2.6	0.65
490	0.7	5.0	5.5	3.1
640	0.8	5.0	7.5	4.0
810	0.9	5.0	11	5.1
1620	0.9	10	40	20.5
V_f0.03				
85	0.8	2.0	2.6	0.67
108	0.9	2.0	3.6	0.85
213	0.8	5	7.5	4.17
270	0.9	5	11	5.25
540	0.9	10	40	21
V_f0.10				
25.6	0.8	2	2.6	0.75
49	0.7	5	5.5	3.75
64	0.8	5	7.5	4.7
81	0.9	5	11	5.75
162	0.9	10	40	23
256	0.8	20	92	75
324	0.9	20	145	92
V_f0.20				
128	0.8	20	92	91
162	0.9	20	145	107

5. Loss modulus – calculation and measurement

Under oscillating stress, rubbery matrix materials dissipate energy, and for small strains the energy W_0 dissipated in each cycle is some fraction h of the peak elastic energy, i.e. $W_0 = h\sigma^2/2E_m$ per unit volume. With discontinuous reinforcement and strong matrix-fibre adhesion the energy W_1 dissipated per cycle in discontinuously reinforced matrix is therefore

$$W_1 = hW_m = V_m(l/4s)^2W_0 \qquad (11)$$

for equal extension of reinforced and unreinforced samples. The loss modulus is thus very readily shown by this energy argument to be greatly increased by reinforcement.

Suppose, however, that instead of matrix and fibre being completely adherent, the fibre-matrix shear bond is weak, so that all the relative displacement between matrix and fibre is accommodated at the interface. The average relative displacement is $\epsilon_m'l/4$. If the sliding frictional force per unit area is τ_f, the energy

dissipated at each fibre during extension ϵ_m' is $\pi(l/r)\tau_f\epsilon_m' l^2/4$ (r is the aspect ratio and l/r therefore the fibre diameter), or four times this amount in one complete cycle of $+\epsilon_m'$ and $-\epsilon_m'$. There are $4V_f/[\pi(l/r)^2 l]$ fibres per unit volume so that the energy dissipated in unit volume during one complete cycle is $4V_f r\tau_f\epsilon_m'$. In addition, hysteresis in the matrix is responsible for a further dissipation of $\frac{1}{2}V_m h\epsilon^2 E_m$ since in each unit volume a sample of volume V_m of matrix undergoes extension of $+\epsilon$ and $-\epsilon$ per cycle. The total energy dissipated by unit volume in a cycle is therefore

$$W_2 = 4V_f r\tau_f\epsilon_m' + \tfrac{1}{2}V_m h\epsilon^2 E_m . \qquad (12)$$

If the fibre-matrix bond is intermediate in strength it may happen that part of the relative displacement is accommodated by sliding and part by shear. Suppose a fraction α is accommodated by sliding. Then the energy dissipated by sliding friction, W_2', becomes $W_2' = \alpha W_2$. A fraction $(1 - \alpha)$ of the relative displacement remains to be accommodated by shear, so that the matrix shear strain is $(1 - \alpha)\epsilon_m' l/2s$ instead of $\epsilon_m' l/2s$. With a linear stress-strain relationship the shear stress is also reduced by the factor $(1 - \alpha)$, so that the hysteresis loss W_1' is $W_1' = (1 - \alpha)^2 W_1$. Hence

$$d(W_1' + W_2')d\alpha = -2(1 - \alpha)W_1 + W_2 ,$$

from which it can be seen that maximum dissipation always occurs at $\alpha = 0$ or $\alpha = 1$. By substituting plausible values for the parameters it seems that $\alpha = 0$ is likely to give larger energy dissipation than $\alpha = 1$. The latter situation is therefore not further considered here.

The composite loss modulus E_c' is defined by

$$\frac{E_c'}{E_c} = \frac{\text{energy dissipated per cycle}}{\text{peak energy stored per cycle}} = \frac{hW_m}{W_c} \qquad (13)$$

using Equation 11. Employing the earlier results for E_c, W_m, and W_c and putting $h = E_m'/E_m$ where E_m' is the loss modulus of unreinforced matrix, it is found that

$$\frac{E_c'}{E_m'} = \frac{V_m(l/4s)^2}{\left[1 + \dfrac{8E_m V_m(l/4s)^2}{15E_f V_f}\right]^2} . \qquad (14)$$

Equation 14 also follows from the elastic-viscoelastic correspondence principle [10] which enables us to replace E_c and E_m in Equation 5 by complex moduli $E_c^* = E_c + iE_c'$ and $E_m^* = E_m + iE_m'$. On resolving the imaginary component Equation 14 is obtained when it is remembered that $E_m'/E_f \ll 1$. The curve of E_c' versus V_f given by Equation 14 is drawn in Fig. 7 using an experimental value for E_m' of 0.041 GN m^{-2}. The loss modulus was also calculated using the shear strain deduced above from Cox's model, by substituting for W_m and W_c in Equation 13 from Equations 8 and 9, and the curve of E_c' versus V_f is drawn in Fig. 7, using the same experimental value ofE_m'. The two calculated lines agree almost exactly. Again the calculations were made down to $V_f = 0.01$ and the curve continued by eye to E_m' at $V_f = 0$.

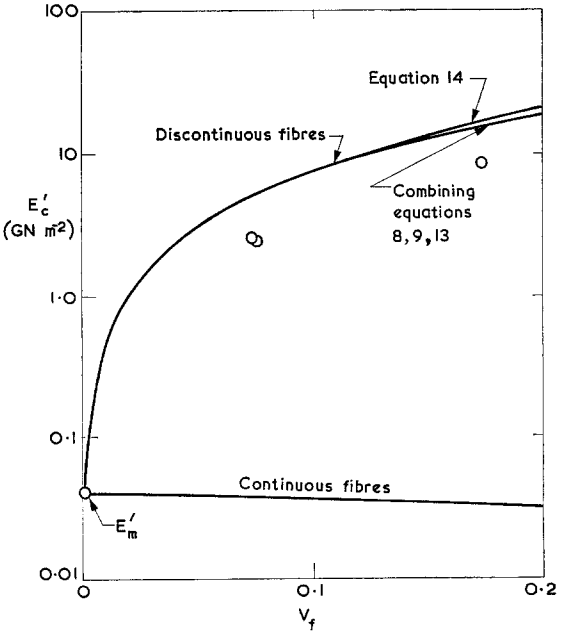

Figure 7 Influence of V_f on longitudinal loss modulus E_c'. The two upper lines are theoretical values for discontinuous fibres, and the lower line is the theoretical result for continuous fibres when $E_f' \ll E_m'$. The circles are experimental measurements. Carbon fibres in soft polymer.

The experimental value of E_m' and the other experimental values in Fig. 7 were obtained by extending the modulus experiments already described on the two-layered steel-polymer or steel-composite strips. At each side of the resonance frequency f_1, the two frequencies were determined at which the measured vibration amplitude was $1/\sqrt{2}$ of the maximum resonance amplitude. The difference between these two frequencies Δf was used to compute E'/E for the

two-layered specimen by the well-known relationship $E'/E = \Delta f/f_1$. The ratio of E'/E for the polymer or composite layer was next calculated from Schwarzl's analysis using the measured thickness ratios of the two-layered strips and $E_s'/E_s = 3.8 \times 10^{-5}$ for steel alone determined by a free-decay method. The calculated loss moduli overestimate the measured values by factors of about 2.

In Fig. 7 the bottom line shows the theoretical loss modulus for continuous reinforcement, i.e. assuming E_c' to be given by the law of mixtures and, of course, no strain amplification within the matrix. In this case $E_c' = V_m E_m'$ if the fibres are perfectly elastic (zero loss). When a large loss modulus is desirable, discontinuous reinforcement is vastly superior to continuous.

6. Design flexibility

In some applications rubber is reinforced with continuous steel wire or continuous polymer fibre. Tyres, belts and hosepipes are examples of this practice. The reinforcement is added to raise the longitudinal tensile breaking strength but also enormously reduces the longitudinal compliance, thus casting away one of the great merits of rubber. Moreover, little variation is possible in the ratio of longitudinal modulus to longitudinal strength.

To show that with discontinuous reinforcement much greater lattitude in the ratio is possible equations for compliance and tensile strength are needed. With continuous reinforcement the compliance C_{cc} is

$$C_{cc} = \frac{1}{E_{cc}} = \frac{1}{E_f V_f} \tag{15}$$

where the subscript cc refers to continuously reinforced composite and the elastic modulus of the matrix has been neglected, which is a reasonable approximation with steel fibres in rubber. The breaking strength σ_b is

$$\sigma_b = \sigma_{fb} V_f \tag{16}$$

where σ_{fb} is the fibre breaking strength and again the matrix contribution has been neglected. From Equations 15 and 16 the ratio of compliance/strength with continuous reinforcement is

$$\frac{C_{cc}}{\sigma_b} = \frac{C_f}{\sigma_{fb} V_f^2}\ , \tag{17}$$

C_f being the fibre compliance, and is invariant with any given matrix and fibre for given composite breaking stress since V_f is then fixed.

Turning to discontinuous reinforcement, in this Section the subscript cd will be used to distinguish it from the continuously reinforced composite. The breaking strength is probably at its highest when the fibres are loaded sufficiently to break first. If the fibre centre stress is, therefore, put at σ_{fb} the average fibre stress is, from Equation 3, $\frac{2}{3}\sigma_{fb}$. Equation 16 is therefore replaced by

$$\sigma_b = \tfrac{2}{3}\sigma_{fb} V_f\ . \tag{18}$$

Thus, one third of the applied load is borne by the matrix. For this result to apply, one condition that must be satisfied is, therefore, $\sigma_b < \frac{1}{3}\sigma_{mb} V_m$, σ_{mb} being the breaking stress of the matrix. In the case of rubber reinforced with steel, σ_{fb} is approximately equal to $10\sigma_{mb}$ so that $V_f \leqslant 0.05$. A second condition is that stress transfer between matrix and fibre must be adequate. It follows from Equation 3 that the fibre-matrix stress τ is a maximum at fibre ends, where it is $\tau = \sigma_{fb}/r$, r being again the aspect ratio of the fibres. A likely value of τ for steel-rubber is 10 N mm^{-2} and of σ_{fb} for steel is 1000 N mm^{-2}, whence $r \geqslant 100$. When these two conditions are satisfied, C_{cd}/σ_b is obtained from Equations 5 and 18 and can be varied a great deal by altering l/s, e.g. by varying the fibre aspect ratio r. A measure of the extra latitude offered by discontinuous reinforcement is given by the range which C_{cd}/C_{cc} can take for a given breaking strength σ_b. From the equations for C_{cc}/σ_b (Equation 17) and C_{cd}/σ_b,

$$\frac{C_{cd}}{C_{cc}} = \frac{2E_f V_f}{3E_m V_m (l/4s)^2} + \frac{16}{45} \tag{19}$$

where V_f is the discontinuous value which = 3/2 times the continuous value.

The value of C_{cd}/C_{cc} for various values of r and V_f has been calculated with $E_f = 2 \times 10^5$ and $E_m = 1$ N mm^{-2}, which are values appropriate to steel and rubber respectively, and the results are plotted in Fig. 8. The tensile strength indicated in Fig. 8 is derived from Equation 18 assuming $\sigma_{fb} = 1000$ N mm^{-2}. Fig. 8 shows e.g. that for a sample breaking strength of 33 N mm^{-2} the compliance can be increased 100-fold if continuous wire reinforcement is replaced by discontinuous. In the manufacture of rubber belting, wire rope is used instead of plain wire in order to improve the compliance; an increase of about two-fold is possible in this way. Compared with such material the discontinuously reinforced rubber sample just referred to has a compliance

50 times larger. Fig. 8 also shows the range of variation of C_{cd} for a given tensile strength for, since C_{cc} is constant with a given V_f (Equation 15), the ordinate shows the wide range of C_{cd} available by altering r. Discontinuous reinforcement thus offers substantial latitude in design of materials like wire-reinforced rubber.

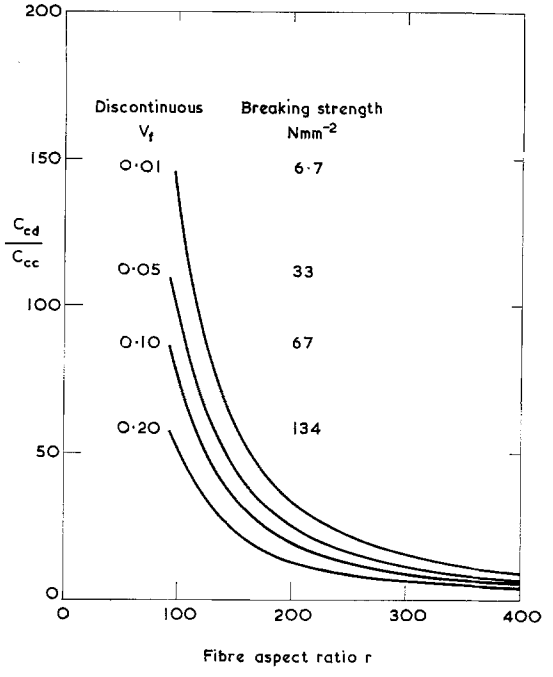

Figure 8 Showing the extra design flexibility offered by discontinuous as against continuous reinforcement. C_{cd} is the compliance of rubber reinforced with steel wires of aspect ratio r. C_{cc} is the compliance of rubber reinforced with continuous steel wires to have the same breaking strength. The ratio C_{cd}/C_{cc} can be very large.

7. Discussion

The information in Fig. 4 shows that the assumption made in calculating with the geometrical model, namely that relative displacement between matrix and fibre increases linearly from fibre centre to fibre end, is reasonably satisfied. The maximum fibre strain cannot exceed $\sigma/E_f V_f$ when the composite strain is σ/E_c; according to Fig. 4, $E_f V_f \sim 7E_c$, so that the fibre strain is everywhere substantially less than the applied composite strain, and when this condition is satisfied the assumption holds. Therefore, it is appropriate to apply the geometrical model to the type of composite under discussion.

For basically the same reason it is not surprising that there is close agreement between the storage modulus as calculated from the geometrical model (Equation 5) and as calculated from the force balance model (Equation 7 or 10). The geometrical argument leading to Equation 5 always gives a fibre stress rising gradually from the fibre end to a rounded peak at the mid-point (Equation 3). The force-balance argument often gives a fibre stress that is almost constant along most of the fibre length and drops rapidly near the fibre end; but here, because $G_m \ll E_f$, and therefore, β is small, the fibre stress distribution is very similar to that deduced from the geometrical argument. Since in this respect the two methods of calculation are similar in this case, they would be expected to give similar values of modulus.

However, both calculations consider only shear strain in the matrix and ignore hydrostatic strain. It is known that in the type of matrix material under consideration shear strain dissipates energy far more effectively than hydrostatic strain. The fact that in Fig. 7 the calculations overestimate the loss modulus suggests that the shear strain has been overestimated, and a reduction by $\sqrt{2}$ in the shear strain used in the calculation would bring the calculated and experimental loss moduli into coincidence. On the other hand, in Fig. 4 such a reduction causes the calculated storage modulus to be only a quarter of the experimental storage modulus; there would be coincidence between the two if hydrostatic strain energy of amount equal to three times the shear strain energy is assumed to be present. Since hydrostatic strain is non-dissipative, the loss modulus would not be affected. As the matrix bulk modulus $= 2G_m(1 + \nu)/3(1 - 2\nu)$ (ν is Poisson's ratio), the hydrostatic strain would then be $\gamma[3(1 - 2\nu)/2(1 + \nu)]^{\frac{1}{2}}$, γ being the shear strain. In rubber-like material $\nu \sim \frac{1}{2}$, so that the hydrostatic strain would be relatively small even though the hydrostatic strain energy is relatively large.

That the shear strain distribution assumed in deriving Equation 5 or Equation 7 should lead to an underestimate of storage modulus (by a factor 2 in Fig. 4) is quite clear from the energy analyses. The assumed distribution necessarily causes holes in the matrix [4] similar to Mileiko's holes [11]. Some additional strain component is needed to ensure that these holes do not exist, and therefore the stored energy and storage modulus are necessarily larger than calculated.

It is in this way that the energy analyses justify the statement in the introduction that they make clear the sense of the approximational error. As just indicated, comparison with the loss modulus is needed to indicate the quantitative division of total strain into shear and hydrostatic strain, although the qualitative existence of hydrostatic strain is evident from the geometrical model [4].

But neglect of some strain component may not be the only reason for a discrepancy between theory and experiment. In the experiments there was a fairly wide range of fibre aspect ratio, while the packing density of fibres would inevitably vary somewhat from place to place. These normal practical factors are reasons why models are only an approximation to reality, and therefore why calculations are unlikely to be in exact agreement with experiment.

It is interesting to compare the present modulus results for fibre reinforcement with those for a material reinforced with spherical particles. The case of a matrix which has linear viscosity and which adheres perfectly to the particles (i.e. no sliding at the matrix-particle interface) has been dealt with many years ago by distinguished authors [12-16], and is continually retreated, e.g. [17]. According to one of the retreatments [18], the viscosity η_p of spherical particles is $\eta_p = \eta(1 + 2.5V_p + 14.1V_p^2)$. Using the Rayleigh analogy to replace this equation concerned with linear viscosity by the equivalent equation concerned with linear elasticity, the effective Young's modulus is

$$E_p = E(1 + 2.5V_p + 14.1V_p^2). \qquad (20)$$

The amplification factor here $(1 + 2.5V_p + 14.1V_p^2)$, is far smaller than the amplification factor of order $(l/4s)^2$ given by strongly adherent fibres.

8. Conclusions

(1) Both experiment and energy analysis indicate that very large increases in axial loss modulus, of order 100-fold, can be obtained by longitudinal reinforcement with discontinuous fibres.

(2) Calculation based on either a geometrical model or a force-balance model *underestimate* storage modulus by a factor of about 2 in the present case of very stiff fibres in a compliant matrix but *overestimate* loss modulus by about the same factor. It is concluded that longitudinal extension of a sample generates a matrix hydrostatic strain, which stores energy non-dissipatively, and which is large enough in the present case to store about three times as much energy as the shear strain does.

(3) Discontinuous reinforcement gives a very much wider choice of compliance for a given breaking strength than does continuous reinforcement.

9. Appendix – the model in Fig. 5

The model prescribes that the wall of the matrix cylinder indicated in Fig. 5 is extended by the amount ϵ, which is the overall composite extension. A plane XYZ then shifts to X'Y'Z'. To calculate the resultant shear stress in the matrix at any point (x, y), start by letting the longitudinal shear stress at the fibre-matrix interface be τ_0, which varies with x. Then at point (x, y) in the matrix the longitudinal shear stress τ is given by $2\pi a\tau_0\,dx = 2\pi y\tau\,dx$ if tensile stresses in the matrix are neglected, as is the case with Cox's model. Then

$$\tau = \tau_0 a/y \qquad (A1)$$

and

$$\gamma = \tau_0 a/G_m y \qquad (A2)$$

where G_m is the matrix shear modulus. Using the standard relation from fibre theory

$$\tau_0 = \frac{a}{2}\frac{d\sigma_f}{dx}$$

and Cox's Equation 31, namely

$$\sigma_f = E_f\epsilon\left[1 - \frac{\cosh\beta(l/2 - x)}{\cosh\beta l/2}\right],$$

Equation A1 becomes

$$\tau = \frac{a^2}{2y}E_f\epsilon\beta\frac{\sinh\beta\left(\frac{l}{2} - x\right)}{\cosh\beta l/2} \qquad (A3)$$

and similarly for γ; ϵ is the longitudinal composite strain as before. Kelly [19] calculates β as

$$\beta = \left[\left(\frac{G_m}{E_f}\right)\frac{2}{a^2\ln(y_1/a)}\right]^{\frac{1}{2}}$$

which agrees with the value Cox gives.

Acknowledgements

We are indebted to D. H. Ferriss for some of the calculations involved in Table I, Dr F. J. Lockett and Mr J. Aveston for useful discussions, and to Mr P. Tattersall of Fothergill and Harvey Ltd, who kindly supplied the mats containing chopped carbon fibres. The work

formed part of the general research programme of the National Physical Laboratory.

References

1. N. F. DOW, General Electric Space Sciences Lab. Report R63SD61 (1963).
2. J. AMIRBAYAT and J. W. S. HEARLE, *Fibre Sci. and Tech.* **2** (1969) 143.
3. H. L. COX, *Brit. J. Appl. Phys.* **3** (1952) 72.
4. D. McLEAN, *J. Mater. Sci.* **7** (1972) 98.
5. G. E. G. BAGG, M. E. N. EVANS and A. W. H. PRYDE, *Composites* **1** (1969) 97.
6. F. SCHWARZL, *Acustica* **8** (1958) 164.
7. E. GOENS, *Ann. Phys. (Leipzig)* **11** (1931) 649.
8. D. H. FERRISS, Conference on Properties of Fibre Composites, National Physical Laboratory – IPC Press (1972) p. 47.
9. J. W. S. RAYLEIGH, "Theory of Sound", Vol. 2 (Macmillan, London, 1896) p. 313; (Dover publications, New York, 1945) p. 313.
10. R. M. CHRISTENSEN, "Theory of Viscoelasticity. An Introduction". (Academic Press, New York and London, 1971) pp. 41-42.
11. S. T. MILEIKO, *J. Mater. Sci.* **5** (1970) 254.
12. A. EINSTEIN, *Ann. Physik.* **19** (1906) 289.
13. HERR BACELIN, quoted in [14].
14. A. EINSTEIN, *Ann. Physik.* **34** (1911) 591.
15. G. B. JEFFREY, *Proc. Roy. Soc.* **A102** (1923) 161.
16. G. I. TAYLOR, *ibid* **A103** (1923) 58.
17. T. B. LEWIS and L. E. NIELSEN, *J. Appl. Polymer Sci.* **14** (1970) 1449.
18. E. GUTH, *J. Appl. Phys.* **16** (1945) 20.
19. A. KELLY, "Strong Solids" (OUP, 1966) p. 126.

Received 1 August and accepted 2 September 1974.